The Temporal Dynamics of Calibration Target Reflectance

Karen Anderson, Edward J. Milton and Elizabeth M. Rollin

School of Geography
University of Southampton
Highfield,
Southampton,
Hampshire, SO17 1BJ,
UK

Email: K.Anderson@soton.ac.uk; E.J.Milton@soton.ac.uk; E.M.Rollin@soton.ac.uk

Abstract

A field experiment investigated the hypothesis that the nadir reflectance of calibration surface substrates (asphalt and concrete) remains stable over a range of time-scales. Measurable differences in spectral reflectance factors were found over periods as short as 30 minutes. Surface reflectance factors measured using a dual-field-of-view GER1500 spectroradiometer system showed a relationship with the relative proportion of diffuse irradiance, over periods when solar zenith changes were minimal. Reflectance measurements were collected over precise points on the calibration surfaces using a novel mobile spectroradiometer device, and uncertainty in terms of absolute reflectance was calculated as being $< 0.05\%$ within the usable range of the instrument (400-1000nm). Multi-date reflectance factors were compared using one-way ANOVA and found to differ significantly ($p = 0.001$). These findings illustrate the anisotropic nature of calibration surfaces, and place emphasis on the need to minimise the temporal delay in collection of field spectral measurements for vicarious calibration or empirical atmospheric correction purposes.

1 Introduction

Earth observation data are increasingly being used to support key decisions by governments and industries for the management of natural resources, with an increasing number of application areas benefiting from the number of platforms and sensors in operation (Slater and Biggar 1996, Teillet *et al.* in press). However, the use of satellite or airborne image data for such purposes is inextricably dependent on accurate absolute radiometric calibration of the sensor, and atmospheric correction of the imagery (Slater 1985). The remotely sensed signal measured by satellite or airborne sensors in the visible and near infra-red (NIR) is strongly

affected by the Earth's atmosphere along the path from the sun to the target surface, and back to the sensor. As a result of sensor-specific factors and temporally variable atmospheric conditions, image digital number (DN) cannot be assumed to represent the actual surface condition (Slater 1980).

It is a widely accepted concept that sensors should be radiometrically calibrated pre-flight or pre-launch in order to derive a relationship between at-sensor digital number (DN) and absolute radiance values (Teillet 1986, Thome *et al.* 1998, Abdou *et al.* 2002). Limitations with this approach are caused by the fact that laboratory calibration sources do not have the colour temperature or the fine spectral structure of sunlight, and hence, reliance solely on pre-launch calibration coefficients can often lead to serious calibration errors (Kieffer and Wildey 1996). On-board calibrators (OBC) are frequently used to monitor the post-launch condition of sensors, but this approach makes the unrealistic assumption that the sensor and OBC devices remain unchanged by the launch, and stable in the outer space environment (Secker *et al.* 2001).

An alternative approach to the post-launch calibration problem is to make reference in-flight to an area on the ground of known spectral radiance (Slater *et al.* 1996). This allows for full optical calibration at a range of brightness intensities, under illumination conditions similar to those used for data acquisition. This method provides an "independent calibration pathway" and is better known as Vicarious Calibration (VC) (Bruegge *et al.* 2001). Where VC and empirical atmospheric correction techniques (i.e. Empirical Line Method) utilise measurements of reflectance at the ground, several surfaces of different albedo are normally used including a dark surface, such as asphalt and a brighter surface such as concrete. The reflectance of these surfaces is often assumed to remain stable over a range of time-scales, and many measurements in support of remote sensing campaigns are made in periods leading up to or following data acquisition, rather than concurrently with the sensor overpass. This paper presents the results of an experiment undertaken at a calibration test-site in the UK, where the main aim was to test the hypothesis that calibration surface reflectance does not change significantly over time.

2 Calibration Site: Thorney Island

Thorney Island is a disused airfield situated in Chichester Harbour, West Sussex, UK. The main focus of previous scientific investigations at this site have centered around the asphalt and concrete runway surfaces at the southern end of the island, which are spatially uniform and provide contrasting albedo (Lawless *et al.* 1998). The site is useful for calibration studies since access to the public is restricted and the runway surfaces remain relatively unused throughout the year. The asphalt site has most recently been used for in-flight calibration of an Itres Instruments Compact Airborne Spectrographic Imager (CASI) (Rollin *et al.* submitted). Figure 1 shows a true colour composite of the site acquired with CASI on 18 June 2002. Three sites on each surface were defined and used in this study, and will be referred to as Thorney Southern Asphalt (TSA 1 to 3) and Concrete (TSC 1 to 3) throughout this paper.

FIGURE 1: True colour composite of Thorney Island calibration site, West Sussex, UK. Collected with CASI operating with the default vegetation bandset (RGB = CASI bands 4,3,2; central wavelengths 670nm, 552nm, 490nm).

3 Methodology

3.1 Field Spectral Measurements

The GER1500 is a dual-field of view (DFOV) spectroradiometer system, measuring cos-conical hemispherical-directional reflectance factors (HDRF) over the visible to near infrared wavelength range (350-1050nm). DFOV spectroradiometric measurements offer the most efficient means of collecting field measurements of spectral reflectance factors since they minimise the temporal delay experienced with a single-beam mode of operation where target and reference measurements are made in sequence (Rollin *et al.* 1998). The precision of DFOV reflectance spectra is known to be strongly dependent on computation of an inter-calibration function, in order to account for differences in the radiant sensitivity and spectral characteristics of the two sensors (Gu *et al.* 1992). Intercalibration measurements were collected several times during each visit to the field site in order to account for temporal changes in the spectral sensitivity of the detector arrays. In the cos-conical configuration, each pair of inter-calibration spectra comprised a measurement of the radiant flux from a calibrated Spectralon panel (target sensor) coupled with a simultaneous measurement of the incident irradiance measured through a cosine corrected diffuser (reference sensor). Throughout this experiment, two calibrated GER1500 spectroradiometers (serial numbers 2002, 2003) were used to measure the HDRF of concrete and asphalt calibration surfaces on five occasions during 2002.

3.2 Spatial Precision in Spectral Measurements

It was necessary to ensure high spatial precision when measuring the calibration surfaces, due to the small field-of-view of the target sensor (3°), combined with localised spatial variations in surface features. In order to achieve this, a mobile spectroradiometer device was designed (Figure 2). The mobile base of the unit allowed ease of movement across the calibration

FIGURE 2: Mobile spectroradiometer device for ensuring positional precision in spectral measurements.

surfaces, and provided a stable mounting point for the spectroradiometers which were fixed to each end of a 3.1m aluminium boom. Tensioned stays were fixed to the base to prevent movement during measurement sequences. In order to position the equipment over the same points on the calibration surface during each visit, the surfaces themselves had to be marked using permanent paint applied in the form of a small cross. Two crosses were painted onto each of the six sites on the concrete and asphalt calibration surfaces and were accurately defined so as to align with the position of two sighting tubes located on the mobile device. The 3° field-of view of the GER1500 sensor head translated to a measurement area of 7.49cm diameter, when the spectroradiometer heads were positioned over the sites at a constant height of 1.43m.

3.3 Meteorological Data

In addition to the spectral measurements, an electronic automatic logging weather station was installed at Thorney Island, in accordance with recommendations for calibration sites suggested by Moran *et al.* (2001) and Teillet *et al.* (2001). The weather station, manufactured by Delta-T Devices, was located within a secure compound owned by the UK Ministry of Defence at the northern end of the Thorney Island main runway. The weather recorder included standard meteorological sensors, plus a digital sunshine sensor manufactured by Delta-T devices (type: BF2), measuring global and diffuse broadband irradiance in the range 400-700nm.

3.4 Analytical Methods

Multi-date reflectance factor measurements made during 2002 were compared using one-way Analysis of Variance (ANOVA) at a range of wavelengths. ANOVA was used to test the null hypothesis that multi-date reflectance samples were drawn from normally distributed

populations with equal means and variances (Fowler and Cohen 1996). Due to the fact that ANOVA is a parametric statistical tool, the multivariate normality of a single sample was tested using a Lilliefors normality test prior to use of the ANOVA statistic. The Lilliefors test was chosen since it makes an adjustment for the fact that the parameters of the normal distribution are estimated from the samples rather than specified in advance, making it more robust than a number of other techniques.

The ANOVA statistic returned an 'F' value which was compared to a lookup table at a given level of significance. The algorithm then provided a probability value, and where this was equal to zero it indicated that at least one sample differed from at least one other sample in the group. It was then necessary to perform a post-hoc Tukey test, for distinguishing where differences were occurring. The Tukey test was used to compare each sample with another at a significance level of $p = 0.001$. The Tukey output statistics provided detail on the sources of statistically significant variation between the population samples.

4 Results

4.1 Uncertainty

The definition of uncertainty is the simple 'quantitative statement on the probability of error', as described by Dungan (2002). In relation to this experiment, a understanding of the inherent uncertainties in the spectral measurement method underpins the quantitative assessment of the results. For this reason, spectral uncertainties on single dates, and spatial uncertainties in multi-date measurements have been estimated.

4.1.1 Within-Date Uncertainties in Reflectance

Uncertainty in single-date reflectance measurements was estimated through analysis of a rapid time sequence of 30 fixed-point reflectance spectra collected under very stable atmospheric conditions on 15 July 2002, at TSA1. For this purpose, the standard deviation (σ_{n-1}) in absolute reflectance and coefficient of variation (CV) in the measurements were used as a measure of uncertainty. CV was calculated using Equation 1:

$$\frac{\sigma_{n-1}}{\overline{x}} \times 100\% \tag{1}$$

Figure 3(a) illustrates that the within-date uncertainty of the method in terms of absolute reflectance is of the order of 0.02% in the range 400-700nm, after which uncertainty increases to a maximum of 0.06% at 1050nm. The increase in uncertainty with wavelength is due to a decline in the signal-to-noise ratio of the instrument at the limits of the detector's spectral range. The CV (Figure 3(b)) exhibits a similar pattern, with spectral variablity increasing to 0.8% at 1050nm, as the signal-to-noise ratio of the instrument's detectors decreases beyond 700nm. In summary, reflectance uncertainty within the usable range of the instrument (400-1000nm) was $< 0.05\%$ in absolute terms, with a CV of less than 0.5%.

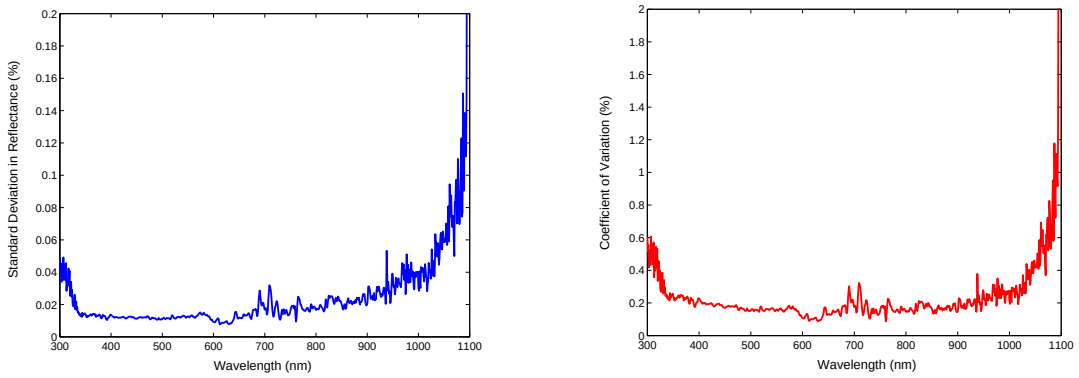

(a) Standard deviation in reflectance (%)

(b) Coefficient of variation (%) in reflectance

FIGURE 3: Reflectance uncertainty of 30 fixed-point asphalt reflectance measurements collected on 15 July 2002 under stable atmospheric conditions.

4.1.2 Between-Date Spatial Positioning Uncertainty

Between-date spatial positioning uncertainty was estimated using a field experiment undertaken on 29 May 2003 at Thorney Southern Asphalt Site 1. The mobile spectroradiometer device was repeatedly positioned over the calibration site markings 32 times, and the position of the trolley fixed using the tensioned stays on each occasion. A sheet of paper was securely fixed to the calibration surface, and following each setting of the trolley the laser pointing device on the target spectrometer head was activated. A pen was used to mark the position of the laser pointer on the paper. This was used as a surrogate measure of the centre of the sensor's field of view.

While the spatial positioning precision of the trolley over the calibration surface markings is estimated as being $\leq$ 5mm in the horizontal (X) and vertical (Y) domains, this translates to a lower positioning precision of the target spectroradiometer head over the calibration surface. This is due to the horizontal separation of the spectroradiometer heads from the trolley, due to the length of the extension pole. The points were digitised and the Root Mean Square Error (RMSE) of the 32 measurements was calculated as being 0.74cm in X and 1.57cm in Y. The spectral uncertainty in between-date measurements due to this spatial uncertainty is currently being investigated, but it is hypothesised that the size of the area measured by the target sensor head (7.49cm diameter) will buffer the effect of these low spatial positioning uncertainties.

4.2 Normal Distribution of Data

Before parametric statistical comparisons of the multi-date spectra could take place, the normality of the data was assessed using a series of 30 fixed point measurements collected under very stable atmospheric conditions on 15 July 2002, at TSA1. Wavelength-dependent variability across the 10-minute time sequence was assessed using a Lilliefors normality test. A value of H=0 from the Lilliefors algorithm indicated that the data could be assumed to

conform to multivariate normality at a significance level of 0.01.

The Lilliefors test highlighted that the data generally conformed to a normal distribution across the wavelength range of the instrument, but at 31 individual wavelengths, deviation from a Gaussian distribution was detected. Of the 31 individual samples highlighted as having non-normal distributions, 24 were located in the wavelength region 300-399nm, where the signal-to-noise ratio of the GER1500 instrument falls off significantly. The remaining wavelengths were 427, 449, 560, 586, 614, 703 and 726nm. These were visually assessed using histograms, and 614nm appeared to conform relatively closely to a Gaussian distribution. 427 and 449nm were found to be affected by outliers, and 560 and 586nm appeared slightly bimodal so were excluded from subsequent ANOVA analysis. 703 and 726nm exhibited a flat distribution, and when compared with other data from the range 700–726nm, a number of other wavelengths exhibited the same pattern, suggesting that this may be a characteristic the asphalt surface in the near infra-red. In addition, the sample size of the data set should be taken into account since it was purposefully small (30 measurements), in order to eliminate reflectance variability caused by changing solar elevation or atmospheric conditions. Ideally, a larger sample collected in a very short time-scale under stable conditions might provide a more suitable data set for normality testing. Overall however, this result demonstrated that the majority of the usable range (400-1000nm) of the GER1500 instrument delivered data conforming to a Gaussian probability distribution, and facilitated further assessment of the data through the use of parametric statistical techniques.

4.3 Short-term Changes in Calibration Target Reflectance

4.3.1 Changes in Asphalt Reflectance on a Single Date

A 30-minute time sequence of reflectance factor measurements collected over a fixed point at TSA on 18 June 2002 showed variation throughout the time sequence. Figure 4 illustrates this variability at 6 wavelengths, chosen since they form the basis of the standardised 'vegetation' bandset used in the CASI airborne imaging system (centre wavelengths of bands 1-6). The same trend in reflectance was found for all other wavelengths measured. These data illustrate that asphalt exhibits a slight but measurable change in absolute reflectance over short time-scales. Due to the low uncertainties in within-date measurements (see Figure 3), these results represent a real change in the surface reflectance factor, rather than a change in instrument sensitivity or measurement position. Analysis of solar zenith changes during the measurement sequence (also Figure 4), revealed that solar elevation changes were minimal, and were unlikely to be the cause of the variation in reflectance. Subsequent analysis of meteorological data, however, showed that the spectral measurement sequence coincided with a period of changing irradiance.

4.3.2 Asphalt Reflectance Factor Responses to Changing Irradiance

The spectral measurement sequence illustrated in Figure 4 coincided with a period of changing global and diffuse irradiance, as shown in Figure 5(a). Meteorological data were recorded at 5 minute intervals and have therefore been interpolated to fit the temporal frequency of the

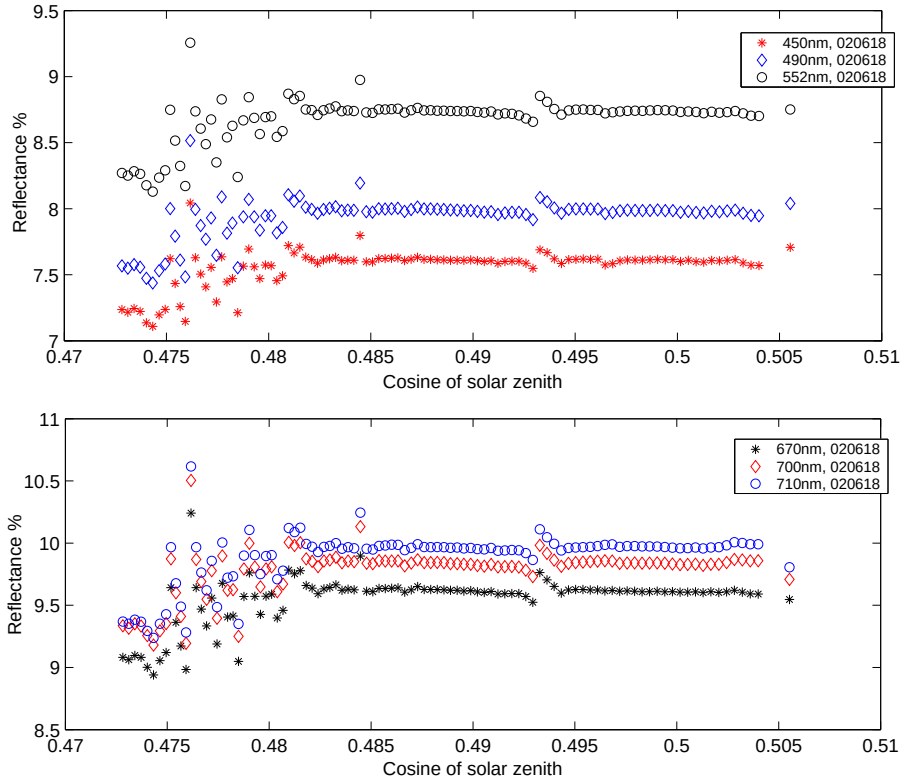

FIGURE 4: Absolute reflectance (%) of TSA in central wavelengths of 6 CASI bands, over a 30 minute time sequence relative to changes in the cosine of the solar zenith angle during this period.

spectral reflectance measurements. Figure 5(a) illustrates that at the start of the measurement sequence, total irradiance was high (1700μmol), with a low diffuse component (270μmol). The diffuse irradiance component increased throughout the sequence to a maximum of 1700μmol at 11:25am. This was coupled with a decrease in the amount of direct irradiance from 834μmol at the start of the sequence to 250μmol by 11:29am.

The diffuse/global (D:G) ratio was used as an indicator of atmospheric clarity, and was correlated with reflectance measured during the 30-minute measurement period. Lower values of the D:G ratio correspond with low atmospheric haze or a lower contribution of diffuse irradiance to the total downwelling light. Values closer to 1 indicate hazier skies with a higher diffuse component. The spectral and meteorological datasets were linked using time stamps within the headers of the spectral data files. This enabled construction of a scatter plot, (Figure 5(b)), where a relationship between reflectance at 670nm (CASI band 4) and the D:G irradiance ratio was apparent ($r^2 = 0.53$). Similar computations were repeated at a range of wavelengths, and all produced similar results.

The general trend apparent in Figure 5(b) suggests that asphalt reflectance increases with increasing sky clarity. This finding corresponds with published results, where the reflectance of natural surfaces has been shown to vary according to changes in the hemispherical distribution of irradiance (Kriebel 1976). The scatter around the trendline may be explained with reference to the interpolation of the weather station data. As previously explained, meteorological

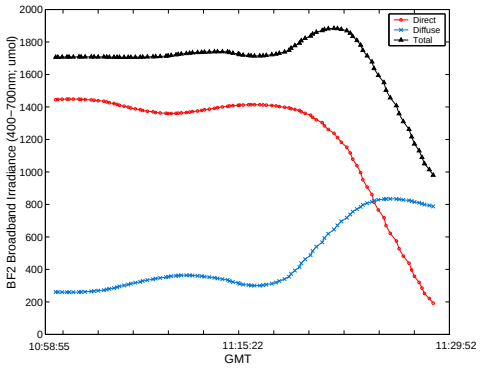

(a) Variability in diffuse, direct and total broadband irradiance (400-700nm) measured over a 30-minute time sequence, corresponding with TSA reflectance measurements on 18 June 2002.

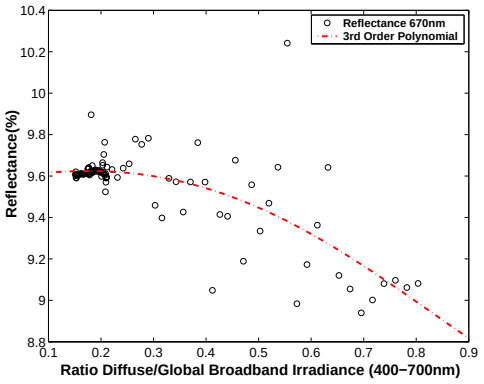

(b) Absolute reflectance (%) of TSA at 670nm and its relationship with diffuse/-global broadband irradiance. Third order polynomial, r^2=0.53.

FIGURE 5: Reflectance variability of an asphalt calibration surface over a 30-minute period, according to changes in the diffuse/global ratio of downwelling irradiance.

data were collected at 5 minute intervals, compared to a 30 second interval used for spectral measurements, and hence some of the scatter evident in Figure 5(b) could be caused by the generalisation effect of interpolation. This will be improved during 2003, where a more rapid logging configuration will be used at the weather station during sequences of spectral measurement collection.

4.4 Longer-term Changes in Calibration Target Reflectance

Reflectance measurements made at TSA1 on 5 separate occasions have been compared using one-way ANOVA at a range of wavelengths. The ANOVA test was then followed by a Tukey test to assess detail in the sources of the between-date variability. The five measurement sequences assessed using this method were collected on: 28 June 2002 (020628); 15 July 2002 (am) (020715am); 15 July 2002 (pm) (020715pm); 29 July 2002 (020729); and 2 September 2002 (020902). The ANOVA algorithm used in this investigation required the number of samples within each population to be equal. Therefore, each sequence of measurements from the asphalt surface were reduced to the size of the smallest sample; resulting in comparisons of five sets of 27 samples at 801 wavelengths. An instrumental problem on 28 June 2002 at all TSC sites resulted in only 9 measurements being collected at TSC1. Therefore, in order to include all five dates into the ANOVA assessment for TSC1, each sequence of measurements was reduced to a size of 9 spectral samples.

Figure 6 and Figure 7 are box and whisker plots describing HDRF reflectance factors measured at 2 wavelengths (550nm, 850nm) for each of the five measurement sequences. These figures represent the original datasets, prior to reduction for use in the ANOVA algorithm. Each box has lines at the lower quartile, median, and upper quartile values. The whiskers are shown as lines extending from each box to show the extent of the remainder of the data. Outliers appear as crosses, and represent data with values falling beyond the ends of the

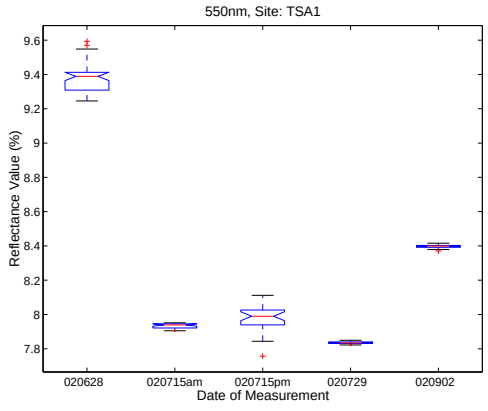

(a) TSA1, 550nm

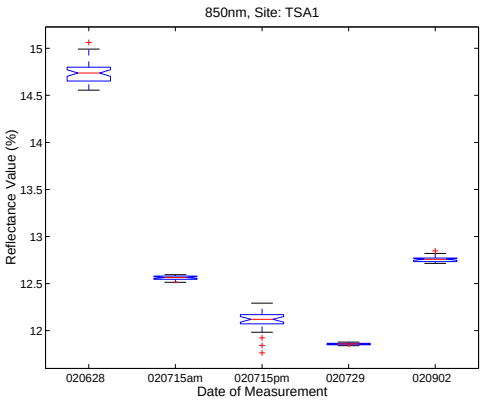

(b) TSA1, 850nm

FIGURE 6: Box and whisker plots illustrating the separability of reflectance factors at TSA1, at (a) 550nm and (b) 850nm measured on five dates. Number of samples: 020628=43; 020715(am)=30; 020715(pm)=27; 020729=30; 020902=36.

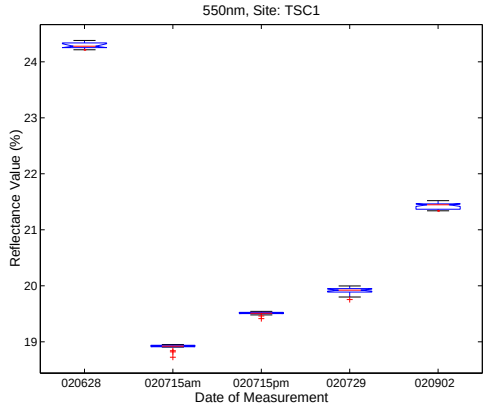

(a) TSC1, 550nm

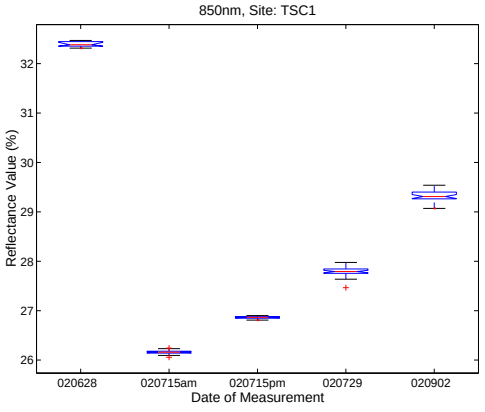

(b) TSC1, 850nm

FIGURE 7: Box and whisker plots illustrating the separability of reflectance factors at TSC1, at (a) 550nm and (b) 850nm measured on five dates. Number of samples: 020628=9; 020715(am)=31; 020715(pm)=30; 020729=30; 020902=28.

whiskers. These plots illustrate only 2 of 801 possible wavelengths, but further computations at multiple wavelengths ensure that the results presented are representative of those across the full spectral range of the GER1500 instrument.

The result of ANOVA computations at a range of wavelengths highlighted that TSA1 reflectance factors measured over the same point on different dates, differed significantly ($p = 0.001$) over time-scales of weeks and months. The same result was found with spectral measurements collected over TSC1 ($p = 0.001$).

4.4.1 Asphalt

For the asphalt site, Figure 6 illustrates that data collected on the two dates with greatest temporal separation (28 June and 2 September 2002) showed significant differences in mean reflectance in the two wavelengths displayed (Tukey $p = 0.001$). This was also true for a range of other wavelengths tested. In addition, reflectance data collected on 28 June and 2 September 2002 showed significant differences in mean reflectance from measurements collected on 15 July (am and pm) and 29 July (Tukey $p = 0.001$). Tukey tests also revealed that the mean TSA1 spectral reflectances measured on 15 July (am and pm) were significantly different from data collected on 29 July 2002, in most, but not all wavelengths ($p = 0.001$). Finally, in some wavelengths, spectra collected in the morning on 15 July were not significantly different from those collected on the same date in the afternoon, as illustrated at 550nm in Figure 6.

4.4.2 Concrete

Figure 7 supports the results of the Tukey test, which reported that reflectance measurements collected at TSC1 showed significant differences in mean reflectance between all five measurement sequences (Tukey $p = 0.001$). This was true for all wavelengths tested. When compared to the reflectance variability of asphalt (Figure 6), concrete appears to exhibit an increased variability in reflectance between dates, in terms of the absolute reflectance measured.

4.4.3 Implications for Calibration Applications

When quantitatively comparing absolute differences between dates in the asphalt and concrete reflectance data (Figures 6 and 7), variation in reflectance at 550nm over the 5 measurement sequences is shown to be of the order of $\pm 3\%$ absolute reflectance in concrete and $\pm 1\%$ absolute reflectance in asphalt. These differences must be viewed in relation to the higher brightness of concrete relative to asphalt. Small changes in asphalt HDRF over longer timescales (Figure 6) are actually of the same order of those in concrete, with a difference of approximately $\pm 6\%$ of the overall reflected signal of both surfaces between the dates in question. Therefore the temporal variability in signal as a proportion of absolute reflectance is similar for both surfaces.

A qualitative assessment of the data suggests that the surfaces may be behaving similarly. For example on 28 June 2002, reflectance of TSA1 and TSC1 were the highest measured values relative to the other four dates. On 15 June and 27 June, the reflectance of both TSC1 and TSA1 fell significantly (Tukey $p = 0.001$). The reflectance of both surfaces exhibited a significant increase in reflectance by 2 September.

These seemingly small changes in calibration target reflectance could have major implications for those utilising field measurements of HDRF for calibration of imaging systems (VC) or empirical atmospheric correction, where a temporal separation exists between collection of ground-based measurements and the sensor overpass. Uncertainties introduced by temporal changes in surface reflectance of the magnitude shown in this paper, could propagate through the calibration process resulting in greater uncertainties in the final calibrated product, thus

placing emphasis on the need to minimise the temporal delay in collection of field spectra in support of calibration programmes.

5 Future Work

Further data collected in early 2003 have been used for preliminary investigation of the relationship between longer-term changes in reflectance relative to the distribution of irradiance. Thus far, only TSA1 has been investigated, but results suggest that longer term trends in reflectance shown in Figure 6, also appear to be related in part, to atmospheric clarity. Some deviations from a perfect linear relationship were found, and may have been caused by surface factors such as moisture or algal growth (Dubosc *et al.* 2001). Solar zenith variations also need to be taken into account. This requires further validation through collection of additional field spectra, scheduled for Summer 2003. Future work will utilise these measurements to develop an empirical model for predicting the behaviour of calibration surfaces under a range of weather conditions, in order to address the uncertainty associated with atmospheric correction or calibration of remotely-sensed data where simultaneous field spectral measurements have not been collected.

6 Conclusions

The results presented illustrate the anisotropic nature of calibration surfaces such as asphalt and concrete. These surfaces have been shown to exhibit measurable changes in reflectance over time-scales as short as 30 minutes, as well as over longer time-scales of weeks and months. Field reflectance factors have been shown to change according to the D:G ratio of downwelling irradiance, with asphalt HDRF exhibiting a general increase with increasing atmospheric clarity. It is concluded that calibration surface reflectance factors cannot be assumed to remain stable over any time period when utilising them for calibration purposes, and the results place emphasis on the need for routine collection of simultaneous diffuse and global irradiance measurements. Research currently in progress aims to address the problem of calibrating historical remotely-sensed datasets, through development of an empirical model to predict the behaviour of calibration surfaces under a range of weather conditions.

Acknowledgements

This work has been funded through a bursary to Karen Anderson, from the John Lewis Partnership Trust, and the Department of Geography at the University of Southampton. The authors would like to thank Bill Damon and Sally-Beth Kelday for technical support throughout this project, and the NERC Equipment Pool for Field Spectroscopy (NERC EPFS) for loan of the GER1500 instrument. Captain Uttley of the Thorney Island 63 Signals Squadron, and Defence Estates are acknowledged for their assistance in gaining access permission to the site.

References

Abdou, W., Bruegge, C., Helmlinger, M., Conel, J., Pilorz, S., Ledeboer, W., Gaitley, B. and Thome, K. (2002). Vicarious calibration experiment in support of the Multi-angle Imaging SpectroRadiometer, *IEEE transactions on Geoscience and Remote Sensing* **40**: 1500–1511.

Bruegge, C., Chrien, N. and Haner, D. (2001). A spectralon BRF database for MISR calibration applications, *Remote Sensing of Environment* **76**: 354–366.

Dubosc, A., Escadeillas, G. and Blanc, P. (2001). Characterisation of biological stains on external concrete walls and influence of concrete as underlying material, *Cement and Concrete Research* **31**: 1613–1617.

Dungan, J. (2002). Toward a comprehensive view of uncertainty in remote sensing analysis, *in* G. Foody and P. Atkinson (eds), *Uncertainty in Remote Sensing and GIS*, John Wiley and Sons, Chichester, UK, pp. 25–35.

Fowler, J. and Cohen, L. (1996). *Practical statistics for field biology*, 6 edn, John Wiley and Sons, Chichester, UK.

Gu, X., Guyot, G. and Verbrugge, M. (1992). Evaluation of measurement errors in ground surface reflectance for satellite calibration, *International Journal of Remote Sensing* **13**: 2531–2546.

Kieffer, H. and Wildey, R. (1996). Establishing the moon as a spectral radiance standard, *Journal of Atmospheric and Ocean Technology* **13**: 360–375.

Kriebel, K. (1976). On the variability of the reflected radiation due to differing distribution of irradiance, *Remote Sensing of Environment* **4**: 257–264.

Lawless, K., Milton, E. and Anger, C. (1998). Investigation of changes in the reflectance of ground calibration targets (asphalt and concrete), *Information for Sustainability: Proceedings of the 27th International Symposium on Remote Sensing of Environment*, ERIM, Ann Arbor, Michigan, pp. 597–600.

Moran, M., Bryant, R., Thome, K., Ni, W., Nouvellon, Y., Gonzalez-Dugo, M., Qi, J. and Clarke, T. (2001). A refined empirical line approach for reflectance factor retrieval from Landsat-5 TM and Landsat-7 ETM+, *Remote Sensing of Environment* **78**: 71–82.

Rollin, E., Emery, D., Kerr, C. and Milton, E. (1998). Dual-beam reflectance measurements and the need for a field inter-calibration procedure, *in* P. Burt, C. Power and P. Zukowskyj (eds), *Developing International Connections: Proceedings of the 24th Annual Conference of the Remote Sensing Society*, Remote Sensing Society, Nottingham, UK, pp. 552–558.

Rollin, E., Milton, E. and Anderson, K. (submitted). Calibration validation of an airborne sensor: an example of the CASI, *International Journal of Remote Sensing (Submitted April 2003)*.

Secker, J., Staenz, K., Gauthier, R. and Budkewitsch, P. (2001). Vicarious calibration of airborne hyperspectral sensors in operational environments, *Remote Sensing of Environment* **76**: 81–92.

Slater, P. (1980). *Remote Sensing - Optics and Optical Systems*, Addison-Wesley, Reading, MA.

Slater, P. (1985). Radiometric considerations in Remote Sensing, *Proceedings of the IEEE* **73**: 997–1011.

Slater, P. and Biggar, S. (1996). Suggestions for radiometric calibration coefficient generation, *Journal of Atmospheric and Ocean Technology* **13**: 376–382.

Slater, P., Biggar, S., Thome, K., Gellman, D. and Spyak, P. (1996). Vicarious radiometric calibrations of EOS sensors, *Journal of Atmospheric and Ocean Technology* **13**: 349–359.

Teillet, P. (1986). Image correction for radiometric effects in remote sensing, *International Journal of Remote Sensing* **7**: 1637–1651.

Teillet, P., Fedosejevs, G., Gauthier, R., O'Neill, N., Thome, K., Biggar, S., Ripley, H. and Meygret, A. (2001). A generalised approach to the vicarious calibration of multiple Earth observation sensors using hyperspectral data, *Remote Sensing of Environment* **77**: 304–327.

Teillet, P., Thome, K., Fox, N. and Morrisette, J. (in press). Earth Observation sensor calibration using a Global Instrumented and Automated Network of Test Sites (GIANTS), *Online Source: Accessed 16th June 2003. http://www.ccrs.nrcan.gc.ca/ccrs/rd/sci_pub/bibpdf/13111.pdf.*

Thome, K., Schiller, S., Conel, J., Arai, K. and Tsuchida, S. (1998). Results of the 1996 Earth Observing System vicarious calibration joint campaign at Lunar Lake Playa, Nevada (USA), *Metrologia* **35**: 631–638.